UNIVERSITY OF FLORIDA

Department of Materials Science and Engineering

132 Rhines Hall
PO Box 116400
Gainesville, FL 32611-6400
(904) 392-1453
Fax: (904) 392-6359

Ph: (352) 392-6664
FAX: (352) 392-4911
E-mail: pholl@silica.mse.ufl.edu

December 15, 1995

Dr. Y.S. Park
Office of Naval Research
800 North Quincy Street
Arlington, VA 22217-5000

Dr. Anis Husain
Defense Sciences Office
ARPA
3701 N. Fairfax Drive
Arlington, VA 22203-1714

Dear Drs. Park and Husain,

      Attached is a progress report summarizing activities in our URI entitled "Blue Light Emitting Materials and Injection Devices" under grant number N00014-92-J-1895. The period summarized is from September 1, 1995 to November 30, 1995.

Sincerely,

Paul H. Holloway
Professor

xc: Dr. A. Goodman
       Dr. Tom Walker
       Dr. Diego Olego

19960501 089

REPORT DOCUMENTATION PAGE

Public reporting burden for this collection of information is estimated to average 1 hour per response, including the time for reviewing instructions, searching existing data sources, gathering and maintaining the data needed and completing and reviewing the collection of information. Send comments regarding this burden estimate or any other aspect of the collection of information, including suggestions for reducing the burden to Washington Headquarters Services, Directorate for Information Operations and Reports, 1215 Jefferson Davis Highway, Suite 1204, Arlington, VA 22202-4302 and to the Office of Management and Budget, Paperwork Reduction Project (0704-0188), Washington, DC 20503

1. AGENCY USE ONLY (Leave blank)	2. REPORT DATE	3. REPORT TYPE AND DATES COVERED
	Dec. 15, 1995	Interim Quarterly Progress Report for September 1, 1995 through November 30, 1995

4. TITLE AND SUBTITLE OF REPORT
Quarterly Progress Report on Visible Light Emitting Materials and Injection Devices.

6. AUTHOR(S)
Paul H. Holloway

5. FUNDING NUMBERS

G: N-00014-92-J-1895

7. PERFORMING ORGANIZATION NAME(S) AND ADDRESS(ES)
University of Florida
Dept. of Materials Science and Engineering
P.O. Box 116400
Gainesville, FL 32611-6400

8. PERFORMING ORGANIZATION REPORT NUMBER:
N/A

9. SPONSORING/MONITORING AGENCY NAME(S) AND ADDRESS(ES)
Office of Naval Research
Dr. Y.-S. Park
800 North Quincy Street
Arlington, VA 22217-5000

10. SPONSORING/MONITORING AGENCY REPORT NUMBER:

11. SUPPLEMENTARY NOTES:

DISTRIBUTION STATEMENT A
Approved for public release
Distribution Unlimited

12a. DISTRIBUTION AVAILABILITY STATEMENT
Unlimited

12b. DISTRIBUTION CODE

13. ABSTRACT (Maximum 200 words)

A report is given on progress of our research into ZnSe-based and GaN-based materials and devices for light emitting diodes and diode lasers.

14. SUBJECT TERMS
Zinc Selenide
Gallium Nitride
Light Emitting Diodes
Diode Lasers

15. NUMBER OF PAGES:
42 + cover

16. PRICE CODE

17. SECURITY CLASSIFICATION OF REPORT:	18. SECURITY CLASSIFICATION OF THIS PAGE	19. SECURITY CLASSIFICATION OF ABSTRACT	20. LIMITATION OF ABSTRACT
Unclassified	Unclassified	Unclassified	Unlimited

ONRCHI COMPUTER V 1.0   11/94   STANDARD FORM 298 (REV 2-89)

GENERAL INSTRUCTIONS FOR COMPLETING SF 298

The Report Documentation Page (RDP) is used in announcing and cataloging reports. It is important that this information be consistent with the rest of the report, particularly the cover and title page. Instructions for filling in each block of the form follow. It is important to *stay within the lines* to meet *optical scanning requirements*.

Block 1. Agency Use Only *(Leave blank)*.

Block 2. Report Date. Full publication date including day, month, and year, if available (e.g. 1 Jan 88). Must cite at least the year.

Block 3. Type of Report and Dates Covered. State whether report is interim, final, etc. If applicable, enter inclusive report dates (e.g. 10 Jun 87 - 30 Jun 88).

Block 4. Title and Subtitle. A title is taken from the part of the report that provides the most meaningful and complete information. When a report is prepared in more than one volume, repeat the primary title, add volume number, and include subtitle for the specific volume. On classified documents enter the title classification in parentheses.

Block 5. Funding Numbers. To include contract and grant numbers; may include program element number(s), project number(s), task number(s), and work unit number(s). Use the following labels:

C	-	Contract	PR	- Project
G	-	Grant	TA	- Task
PE	-	Program Element	WU	- Work Unit Accession No.

Block 6. Author(s). Name(s) of person(s) responsible for writing the report, performing the research, or credited with the content of the report. If editor or compiler, this should follow the name(s).

Block 7. Performing Organization Name(s) and Address(es). Self-explanatory.

Block 8. Performing Organization Report Number. Enter the unique alphanumeric report number(s) assigned by the organization performing the report.

Block 9. Sponsoring/Monitoring Agency Name(s) and Address(es). Self-explanatory.

Block 10. Sponsoring/Monitoring Agency Report Number. *(If known)*

Block 11. Supplementary Notes. Enter information not included elsewhere such as: Prepared in cooperation with...; Trans. of...; To be published in.... When a report is revised, include a statement whether the new report supersedes or supplements the older report.

Block 12a. Distribution/Availability Statement. Denotes public availability or limitations. Cite any availability to the public. Enter additional limitations or special markings in all capitals (e.g. NOFORN, REL, ITAR).

DOD - See DoDD 5230.24, "Distribution Statements on Technical Documents."
DOE - See authorities.
NASA - See Handbook NHB 2200.2.
NTIS - Leave blank.

Block 12b. Distribution Code.

DOD - Leave blank.
DOE - Enter DOE distribution categories from the Standard Distribution for Unclassified Scientific and Technical Reports.
NASA - Leave blank.
NTIS - Leave blank.

Block 13. Abstract. Include a brief *(Maximum 200 words)* factual summary of the most significant information contained in the report.

Block 14. Subject Terms. Keywords or phrases identifying major subjects in the report.

Block 15. Number of Pages. Enter the total number of pages.

Block 16. Price Code. Enter appropriate price code *(NTIS only)*.

Blocks 17. - 19. Security Classifications. Self-explanatory. Enter U.S. Security Classification in accordance with U.S. Security Regulations (i.e., UNCLASSIFIED). If form contains classified information, stamp classification on the top and bottom of the page.

Block 20. Limitation of Abstract. This block must be completed to assign a limitation to the abstract. Enter either UL (unlimited) or SAR (same as report). An entry in this block is necessary if the abstract is to be limited. If blank, the abstract is assumed to be unlimited.

Quarterly Progress Report

September 1, 1995 to November 30, 1995

Visible Light Emitting Materials and Injection Devices

ONR/ARPA URI

Grant Number N00014-92-J-1895

Prepared by:

Paul H. Holloway
Department of Materials Science and Engineering
University of Florida
P.O. Box 116400
Gainesville, FL 32611
Ph: 352/392-6664; FAX: 352/392-4911
E-Mail: Internet - pholl@silica.mse.ufl.edu

Participants:
University of Florida
Kevin Jones
Robert Park
Joseph Simmons
Cammy Abernathy
Stephen Pearton
Dept. of Materials Science and Engineering
Timothy Anderson
Dept. of Chemical Engineering
Peter Zory
Dept. of Electrical Engineering
Columbia University
Gertrude Neumark
Dept. of Materials Science and Engineering
Oregon Graduate Institute of Science and Engineering
Reinhart Engelmann
Dept. of Electrical Engineering

(I)   MOMBE Growth and Doping of Column III-Nitride Materials (Cammy Abernathy and Steve Pearton)

Minority Carrier Enhanced Reactivation of Hydrogen-Passivated Mg in GaN

The influence of minority carrier injection on the reactivation of hydrogen passivated Mg in GaN at 175°C was investigated in p-n junctions. The dissociation of the neutral MgH complexes is greatly enhanced in the presence of minority carriers and the reactivation process follows second order kinetics. Conventional annealing under zero-bias conditions did not produce Mg-H dissociation until temperatures >450°C. These results provide an explanation for the e-beam induced reactivation of Mg acceptors in hydrogenated GaN. The acceptor passivation and reactivation reactions can be represented by:

$$(AH)^o \rightarrow A^- + H^+$$
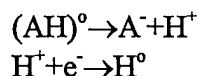$$H^+ + e^- \rightarrow H^o$$

Fig. I.1 shows a series of acceptor concentration profiles measured in the same p-n junction sample, after annealing at 175°C under forward bias conditions. After the hydrogenation treatment the electrically active acceptor density decreased by a factor of approximately two. If the subsequent annealing was carried out in the open circuit configuration there was no change in the carrier profile for periods up to 20 hr at 175°C. By sharp contrast, for increasing annealing times under minority carrier injection conditions (i.e. forward bias of the junction) there was a progressive reactivation of the Mg acceptors with a corresponding increase in the hole concentration. The Mg reactivation has a strong dependence on the depth into the p-type layer, which may result from the diffusion distance of the injected electrons prior to recombination.

The fact that the MgH complexes are unstable against minority carrier injection has implications for several GaN-based devices. In a laser structure the high level of carrier injection would rapidly dissociate any remaining MgH complexes and thus would be forgiving of incomplete removal of hydrogen during annealing. In an HBT, the lower level of injected minority carriers would also reactivate passivated Mg in the base layer, leading to an apparent time-dependent decrease in gain as the device was operated.

Hydrogen Passivation of Ca Acceptors in GaN

We recently realized p-type doping of GaN using implantation of Ca, followed by annealing at >1100°C. The activation efficiency was ~100% ,but the ionization level was found to be ~168 meV, which is similar to that of Mg. The Ca profile was thermally stable at temperatures up to 1125°C. Since Mg has a substantial memory effect in stainless steel reactors, Ca may be a useful alternative p-dopant for epitaxial growth of laser diode or HBT structures in which junction placement and hence control of dopant profiles, is of critical importance. As shown in Fig. I.2 , exposure to a hydrogen plasma at 250°C leads to a reduction in sheet carrier density of approximately an order of magnitude. The hole mobility increased from 6 to 18 cm^2/V-sec. The process was reversible by post-hydrogenation annealing at 400-500°C under a N$_2$ ambient, and is characteristic of the formation of neutral Ca-H complexes in the GaN. The thermal stability of the passivation is similar to that of Mg-H complexes in material prepared with similar initial doping levels.
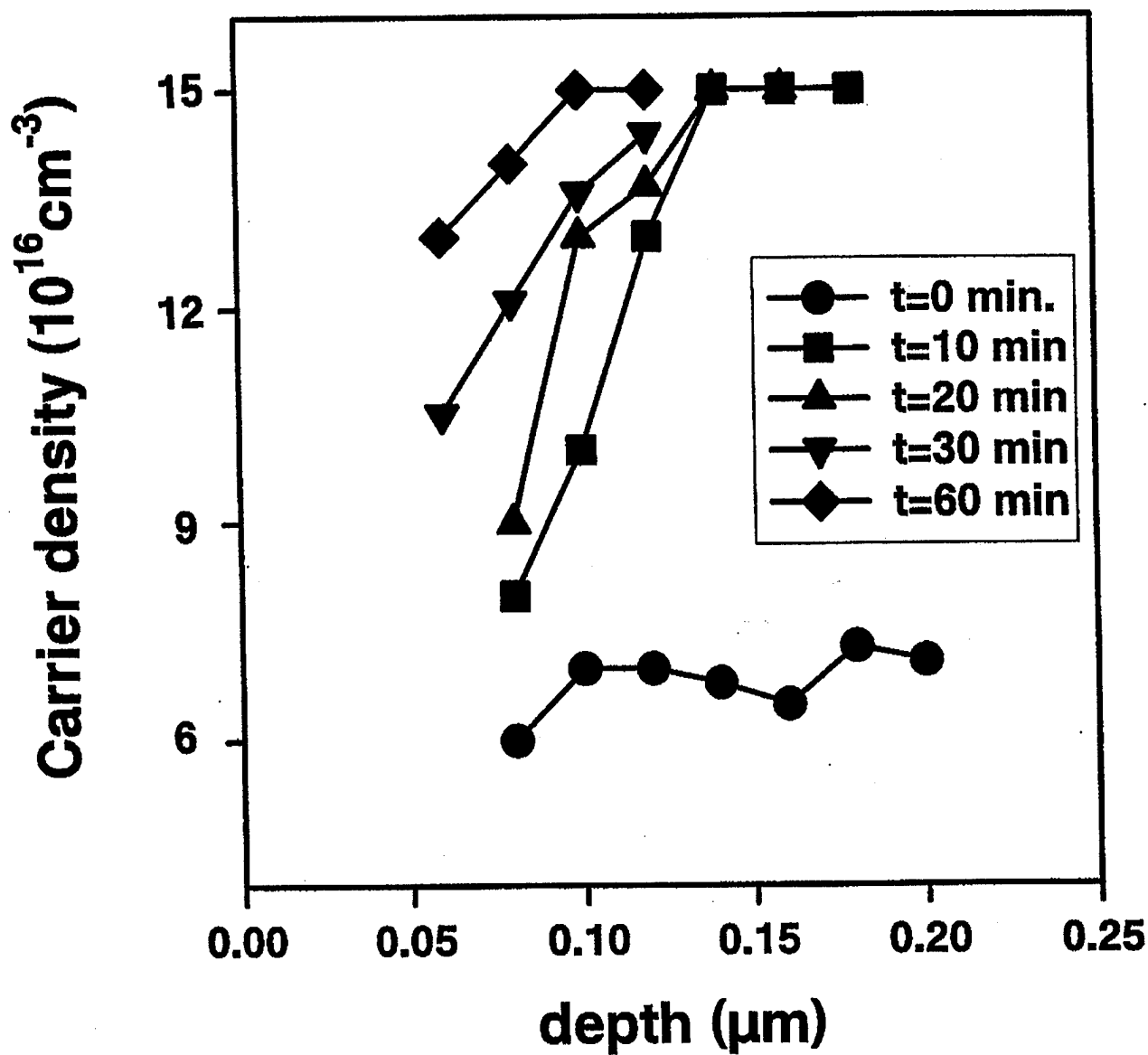
Fig. I.1.   Carrier concentration profiles in hydrogenated GaN(Mg),after annealing
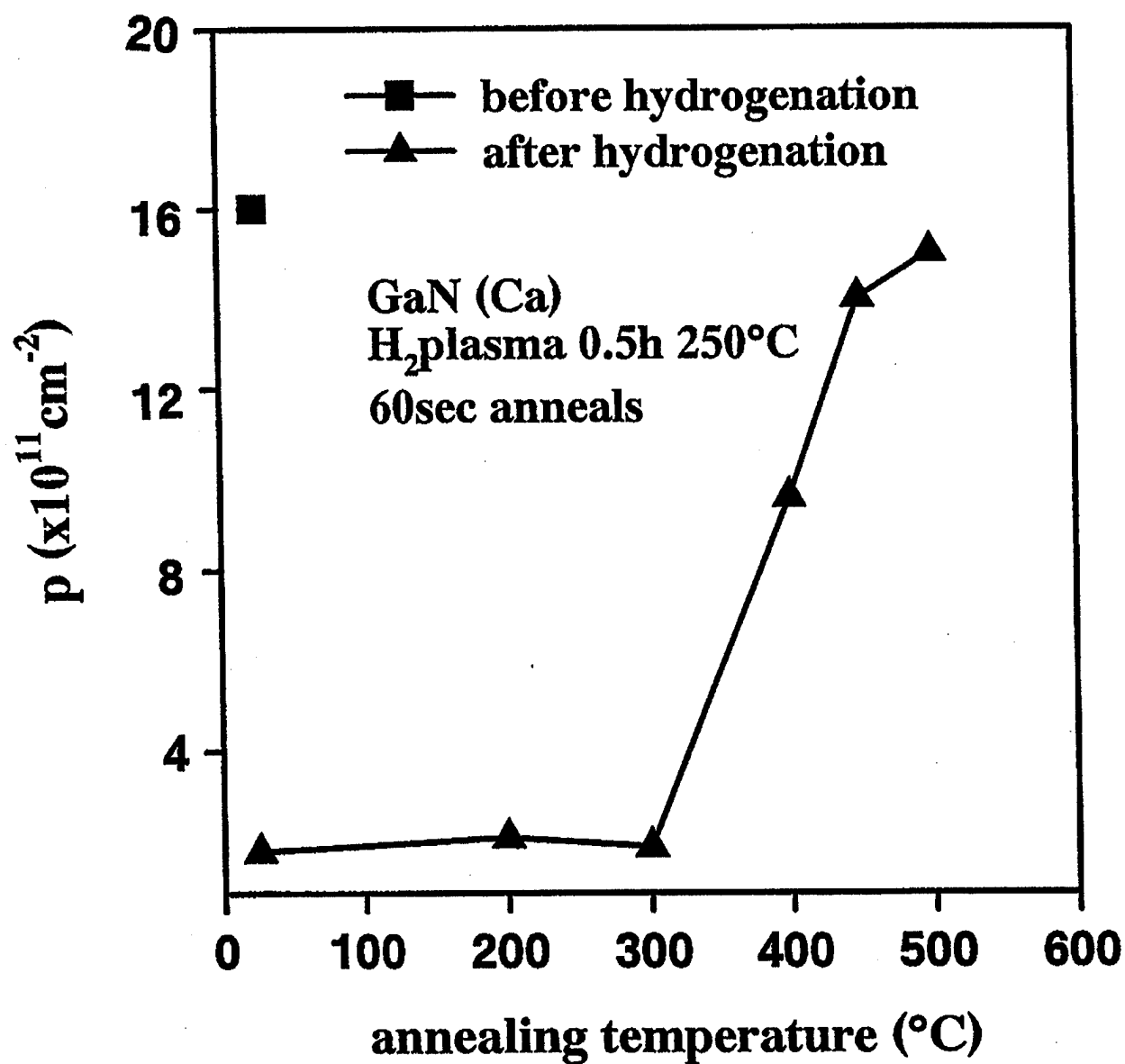for various times at 175°C under forward bias conditions.

Fig. I.2. Sheet hole density at 300K in hydrogenated GaN (Ca) as a function of subsequent annealing temperature.

Ca and O Ion Implantation Doping of GaN.

P- and n-type doping of GaN has been realized by ion implantation of Ca and O, respectively. Fig. I.3 shows that both Ca and Ca+P implanted samples convert from n-type to p-type after a 1100°C anneal. Under the same conditions, the unimplanted sample remains n-type with a slight decrease in sheet resistance that may result from the creation of additional N-vacancies or the depassivation of other n-type impurities. Fig. I.4 shows that the ionization level for Ca of 169 meV is similar to that of Mg. Fig. I.5 shows that implanted O displayed an ionization level of 29 meV. Using these values, we can estimate activation efficiencies of ~100% for Ca, but only 3.6% for O. Note that the unimplanted and annealed material has an activation energy for conduction of 335 meV.

Fig I.6 shows the SIMS profiles for as-implanted and annealed (1125°C, 15 sec) Ca in GaN. There is no measurable redistribution of the dopant. Similar results are shown in Fig I.7 for O-implanted material. Based on a conservative estimate of the resolution of the SIMS instrument, an upper limit of 2.7×10^{-13} cm^2/sec is estimated for the diffusivity of both Ca and O in GaN at 1125°C.

(II)   Ohmic Contacts (Paul Holloway)

Degradation of Au/Pd/ZnTe-ZnSe MQW Ohmic Contacts to p-ZnSe

Analysis of electrically degraded multiquantum well (MQW) contacts indicates that localized Joule heating results in localized contact failure at the point at which power is supplied to the structure. The dimensions and composition of the probe used to supply power is a critical parameter in this failure, since localized temperatures increase as the probe size decreases leading to higher localized current densities and heating. Localized heating results in diffusion of Zn and Te from the ZnTe layer to the sample surface. In addition, alloying occurs between the Au and Pd layers. In longer degradations (90 minutes), Zn from the underlying ZnSe layer also diffuses to the sample surface resulting in a disruption of the stoichiometry of the ZnSe. The diffusion and alloying were found to occur for current densities as low as 40 A/cm^2. Diffusion and alloying were prevented only when the sample was cooled to ~15 °C or less during degradation.

At higher current densities ($\approx$1000 A/cm^2), the thermal stresses generated by the localized heating were sufficient to result in the formation of micro-cracks. The micro-cracks were from ~0.5 to 5 mm in length and extended through the multiquantum well contact and into the GaAs substrate. The cracks were found to lie along the <100> directions and are believed to occur on the {110} cleavage planes. By using a Cu probe to degrade the contacts (as opposed to an Au probe), Cu was introduced as an impurity into the sample structure. Analysis of the samples and diffusion calculations indicate that the micro cracks act as high diffusivity paths for Cu, and potentially for other impurities.

In addition, rectangular features formed symmetrically around the micro-cracks. The geometry and orientation of the rectangular features are similar to the dark line defects (DLDs) which form in degraded quantum well ZnSe-based diode lasers. DLDs and the rectangular features are also similar in that the DLDs are dislocation which act as high diffusivity paths for point defects, and the rectangular features form around micro-cracks which act as high diffusivity paths for impurities. Also, DLD formation is believed to be
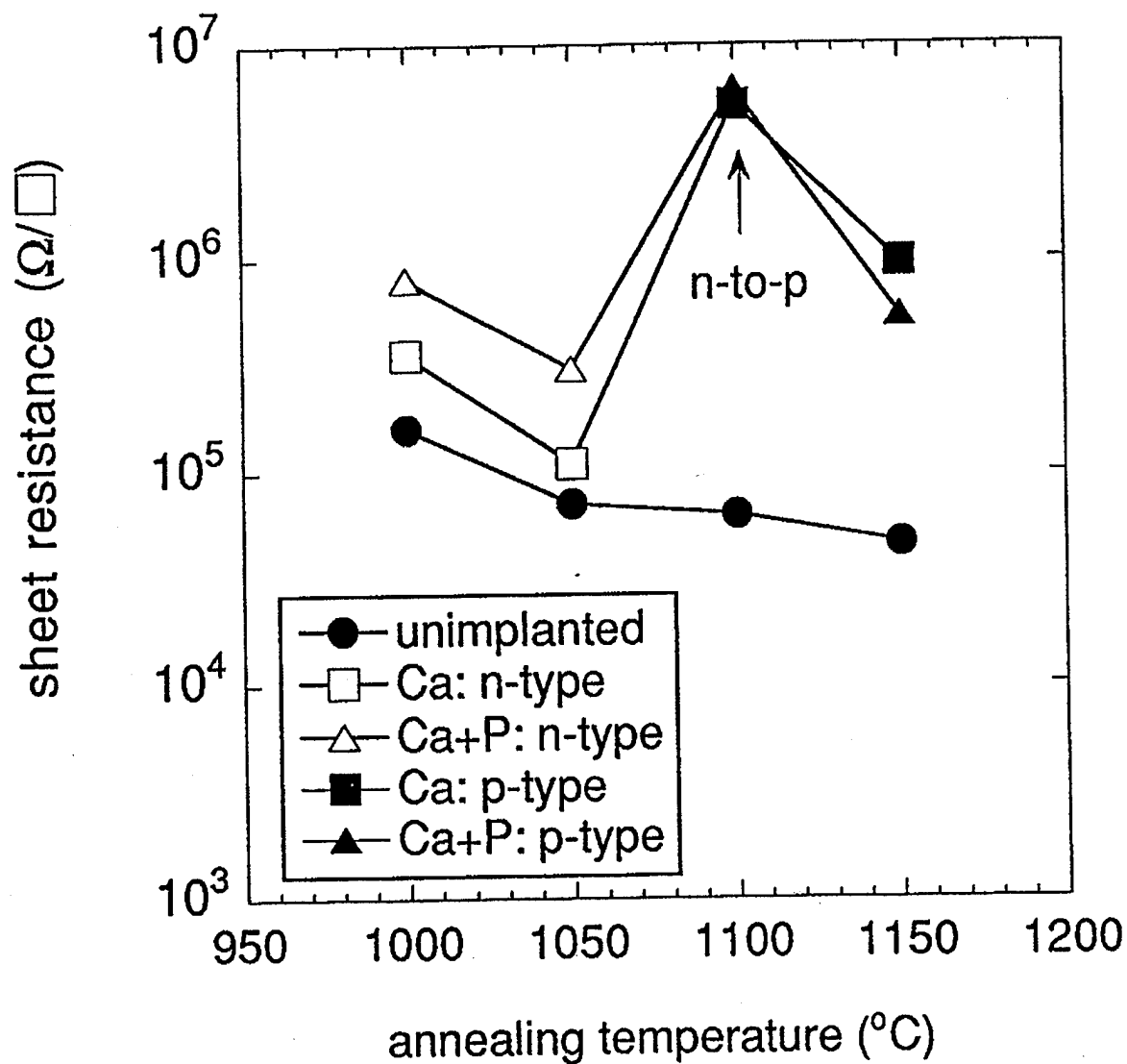
Fig. I.3.   Sheet resistance versus annealing for GaN either unimplanted or implanted with Ca or Ca+P. The implanted samples convert from n-type to p-type after a 1100°C anneal.
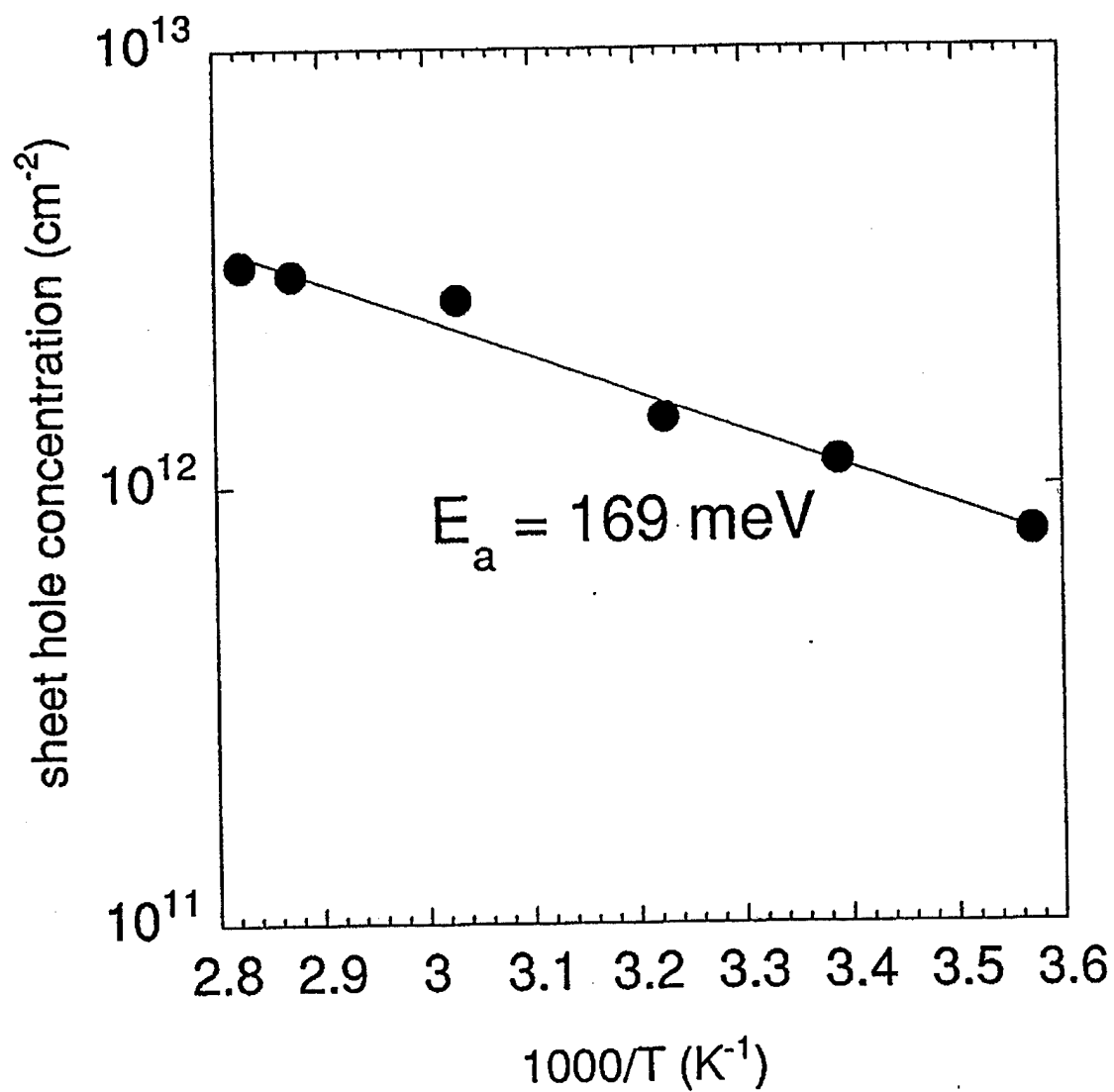
Fig. I.4.   Arrhenius plot of the sheet hole concentration for Ca-implanted GaN annealed at 1150°C.
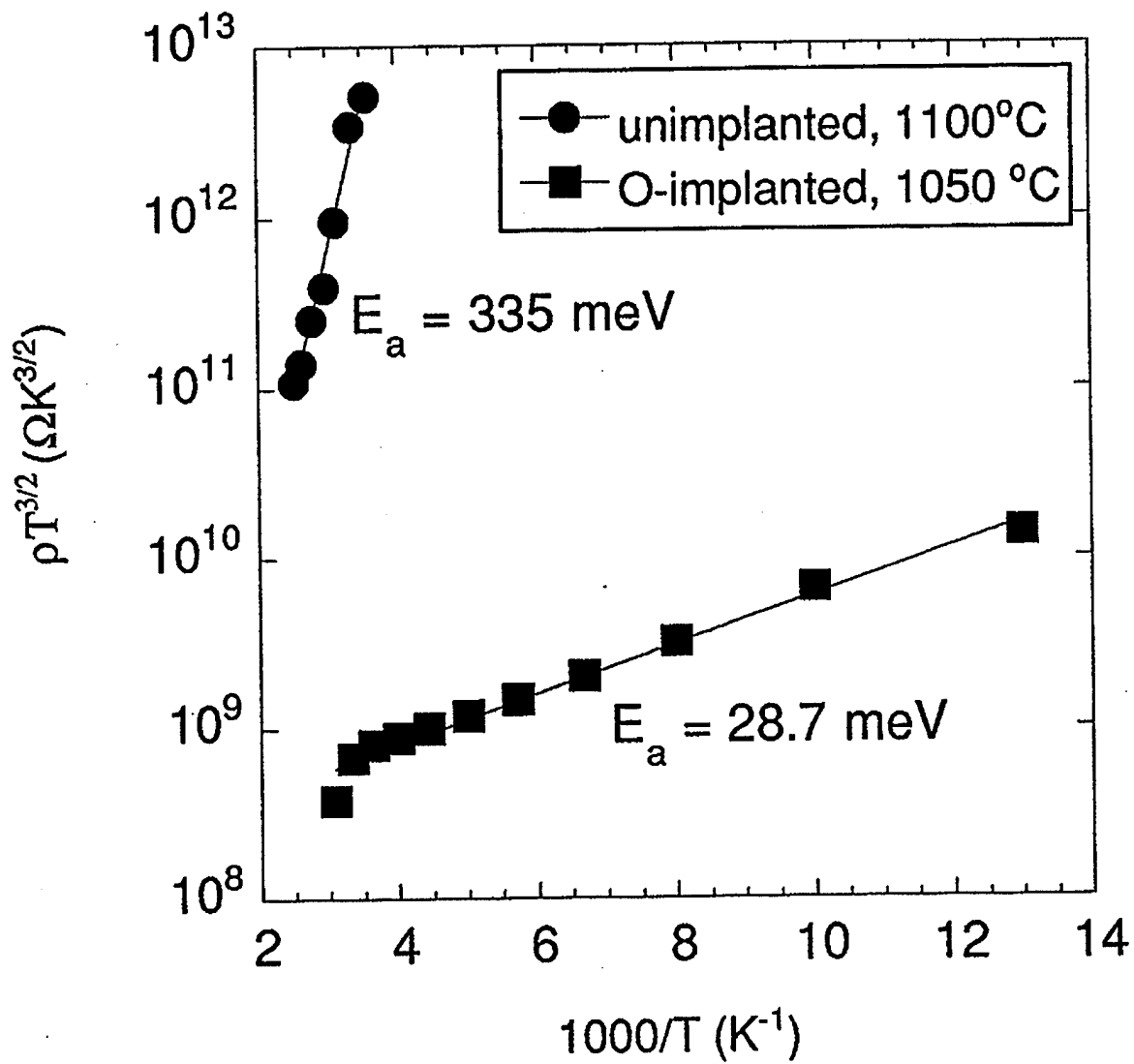
Fig. I.5.   Arrhenius plot of the resistance /temperature product for unimplanted GaN annealed at 1100°C and O-implanted GaN annealed at 1050°C.
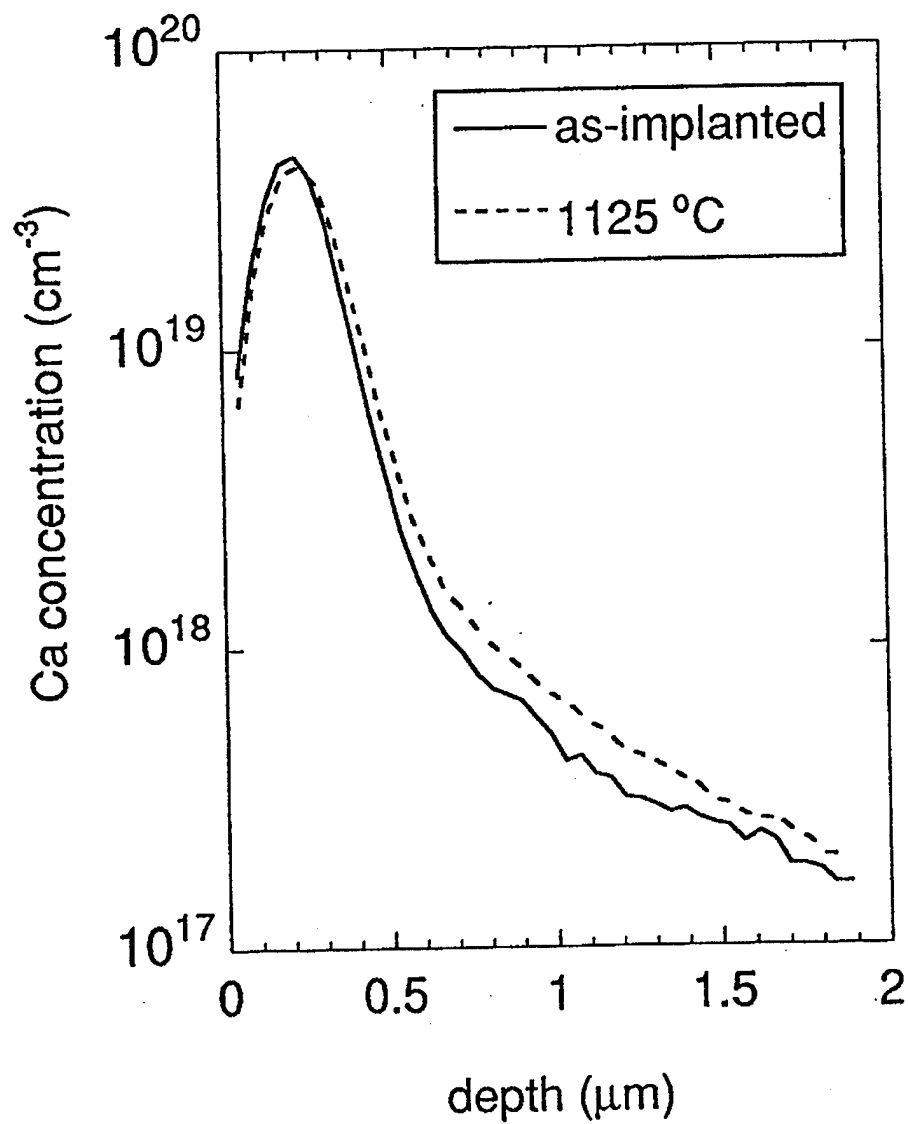
Fig. I.6.   SIMS profile of Ca-implanted GaN before and after annealing at 1125°C.
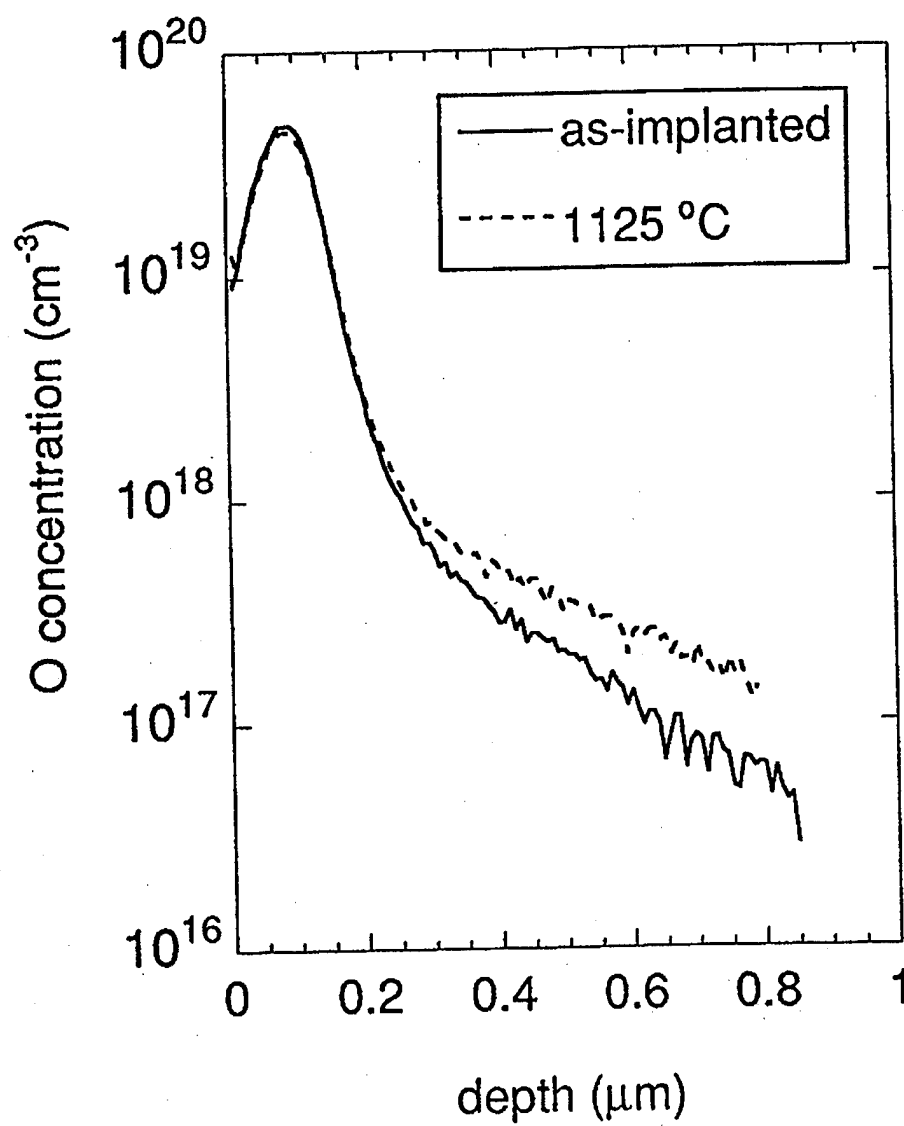
Fig. I.7.   SIMS profile of O-implanted GaN before and after annealing at 1125°C.

accelerated by localized heating from non-radiative recombinations, while the rectangular feature's form as a result of localized Joule heating. Finally both the quantum well region of the lasers and MQW are highly stressed, leading to point defects diffusion. Due to these similarities, the rectangular features are believed to result from dislocation patches in the MQW contacts which are similar to the patches of DLD dislocations in the quantum well of diode lasers.

Ohmic Contacts to p-ZnTe

Studies of the formation of ohmic contacts to p-ZnTe using Au metallizations were completed. The as-deposited contacts were rectifying, but heating for 15 minutes at T = 150°C resulted in ohmic behavior. Resistance increases were observed for longer times at all temperatures, with large increases following heat treatments at 350°C. AES and SIMS data showed diffusion of Au into the p-ZnTe layer at 250°C, which led to acceptor-doping of ZnTe and therefore increased conductivity through the near surface layer. Diffusion of Au was extensive and a ternary Zn-Te-O compound was formed at 350°C, leading to degradation of the contact properties. Also, the surface of the contact became very rough at 350°C, from "balling up" of the metallization on ZnTe. This work has been submitted for publication.

Ohmic Contacts to p-GaN

Ohmic contact metallizations of Au, Au/Ni, and Au/C/Ni to p-GaN were investigated using I-V measurements, AES, and SIMS. The 200 nm thick single metal Au contacts were DC magnetron sputter deposited, while the other metallization schemes (100 nm Au/50 nm Ni and 100 nm Au/10 nm C/50 nm Ni) were electron beam evaporated. The as-deposited Au contacts were rectifying, and they remained rectifying even after heat treatment to temperatures up to 600°C for times up to 30 minutes. AES data showed that the Au did not penetrate into the GaN lattice upon annealing.

The as-deposited Au/Ni contacts were also rectifying, but exhibited nearly linear I-V data after annealing at 400°C for 5 minutes. AES and SIMS data both showed evidence of Ni diffusion into the p-GaN matrix and also throughout the Au contact layer. It was postulated dissociation of the GaN matrix by Ni provided the opportunity for carbon p-type doping of the near surface region of the p-GaN, leading to increased conduction. AES data showed an increased carbon concentration at the metal/p-GaN interface from contamination prior to contact metallization, and this was postulated to be the source of dopant C. A mechanism was proposed in which dissociated GaN regrows at the interface, with the driving force for regrowth being the formation of a Au-Ni solid solution. A 10 nm thick carbon layer was deposited between the Au and Ni in an attempt to increase the doping of the near-surface region of the GaN. Unfortunately, the doping level remained nearly the same. This may indicate that the carbon concentration in the GaN is saturated at the level of contamination, and even that the C may act as an amphoteric dopant and compensate acceptor levels at high concentrations.

10

(III)   Degradation Study of II-VI LEDs (Kevin Jones)

Relaxation of strain in ZnSe quantum wells used in LEDs and diode lasers was investigated using low temperature PL, electroluminescence (EL) microscopy and transmission electron microscopy (TEM).   LEDs were fabricated from a separate confinement heterostructure (SCH) with a single quantum well (ZnCdSe QW/ZnSSe/ ZnMgSSe/GaAs) and degraded by applying an electrical current. Strain in the quantum well region was estimated by monitoring the PL exiton peak positions. The strain in the quantum well remained constant until greater than 60% degradation, i.e. until the emitted light intensity decreased to 40% of the initial intensity. Even at this level of degradation, dark line defects had evolved into a network as observed by EL. However, the strain in the quantum well did not relax until after 80% degradation to about 1/3 of the initial value. These results indicate that the strain in the quantum well region may not be directly responsible for DLD formation during the early stages of degradation , but it may contribute to degradation at a later stage. Also, the results indicate that the <100> dark line defects that are usually observed after degradation are not a result of strain relaxation. They probably result from point defect agglomeration. Pre-existing defects, such as misfit dislocation, threading dislocations, and/or stacking faults may act as nucleation sites for these degradation-induced defects.

(IV)   Optical and Electrical Characterization of ZnSe (J.H. Simmons)

During the past year, we have set up a short-pulse laser spectroscopy system capable of conducting carrier lifetime measurements on semiconductor quantum well structures. In cooperation with Dr. R. Park and M. H. Jeon, who fabricated the appropriate quantum well structures of $Cd_xZn_{1-x}Se/ZnSe$ (x=0.2), we have studied the photoluminescence and photo-excited carrier dynamics in wells with differing barrier widths and well thicknesses.

The results have been analyzed and are being published in several parts. The first, to be described here, appeared in Applied Physics Letters. In this work, we have analyzed the positions of the photoluminescence spectra of a $Cd_xZn_{1-x}Se/ZnSe$ (x=0.2) quantum well structure consisting of a GaAs substrate, followed by a 2 μm ZnSe buffer layer, then 10 periods of undoped $Cd_{0.2}Zn_{0.8}Se/ZnSe$ quantum wells with a barrier thickness of 100 Å, and a well thickness of 50 Å. The electron-hole states of the structure were measured by absorption spectroscopy and by low temperature photoluminescence, and were calculated using an envelope wave function approximation with a tight-binding expansion developed by Bastard.

The photoluminescence spectra clearly show an intensity dependent spectrum with two distinct peaks. The high energy peak (see article in the appendix) is proportional to the incident intensity and corresponds to the exciton recombination process, while the low energy peak corresponds to the biexciton process. The latter assignment was uniquely made for the first time in this system by using a number of tests which prove conclusively that the peak is a biexciton peak. These tests consist of: (1) comparison of energy position with calculated positions based on the tight-binding calculation referenced above and on the position of absorption features in a similar film deposited on a ZnSe substrate, (2) the

11

demonstration of a quadratic dependence of peak intensity on incident light intensity, (3) the lineshape of the spectral feature which shows reverse Boltzmann statistics expected of a bi-exciton transition, (4) the observation of a lifetime for the low energy peak which is nearly half the lifetime of the exciton feature, and most importantly, (5) the polarization dependence of the low energy peak which shows biexciton formation only when cross polarized beams are used, and no biexciton feature when co-circular polarized beams are used. Only biexcitons can exhibit the latter feature through the constraints of opposite spin addition in the coalescence of two excitons.

The conclusive demonstration of a biexciton peak gives a binding energy of 14 meV for the biexciton peak. This peak position agrees exactly with the position of the low temperature ZnSe laser emission. This suggests that, contrary to papers attributing the lasing process to modified electron-hole plasmas or exciton related processes, the *low temperature* lasing mechanisms in these materials is clearly a biexciton process.

Studies of the effect of well thickness and barrier thickness on the behavior of the low temperature exciton and biexciton processes are being conducted to determine the carrier dynamic mechanisms in these structures. Also under study is the mathematical description of biexciton gain. The same emission data are being collected at room temperatures to determine the high temperature mechanisms which govern the behavior of these materials. Finally studies are also under way of photoinduced structural damage to determine how the lasing-induced structural defects affect the free carrier dynamics and the gain process and eventually result in quenching of lasing activity.

Also during the past quarter, we have measured the photoexcited carrier lifetimes in ZnSe quantum wells at 10K grown on GaAs and on ZnSe substrates. The results are being analyzed, but preliminary photoluminescence data shows both exciton and biexciton transitions with lifetimes of 266 and 108 ps, respectively. We are measuring the effect of barrier width on the behavior of their lifetimes.


(V)   MOCVD Growth of $Zn_{1-x}Cd_xS$ and GaN Thin Films (Tim Anderson)

$Zn_{1-x}Cd_xS$ Thin Films

We have continued this quarter to optimize the MOCVD growth conditions for the $Zn_{1-x}Cd_xS$ thin films on GaAs substrates for potential laser applications. New sulfur source MSH (methyl mercaptan) has been tested. According to the literature, this precursor eliminates pre-reactions with Group II MO-sources. We have shown that MSH, along with DEZn and DMCd sources, can successfully be used as precursors to grow good quality $Zn_{1-x}Cd_xS$ films in the 500-700° C temperature range.

The effects of growth temperature, component flow rates, and their gas phase ratio on the carrier type, quality of crystal structure, and the composition of $Zn_{1-x}Cd_xS$ films have been examined. Fig. V.1 shows the dependence of the composition and crystal quality upon temperature. It shows that increasing temperature improves the crystallinity of the zinc-blende type films and decreases the amount of Cd incorporated in the samples. This result is consistent with the higher vapor pressure of CdS. At a temperature close to 700°C, the growth rate drops significantly, thus narrowing the optimal deposition temperature to 600-650° C. It also has been shown that the gas-solid distribution

Fig. V.1. Composition x and structural quality
of the $Zn_{1-x}Cd_xS$ films vs growth temperature.
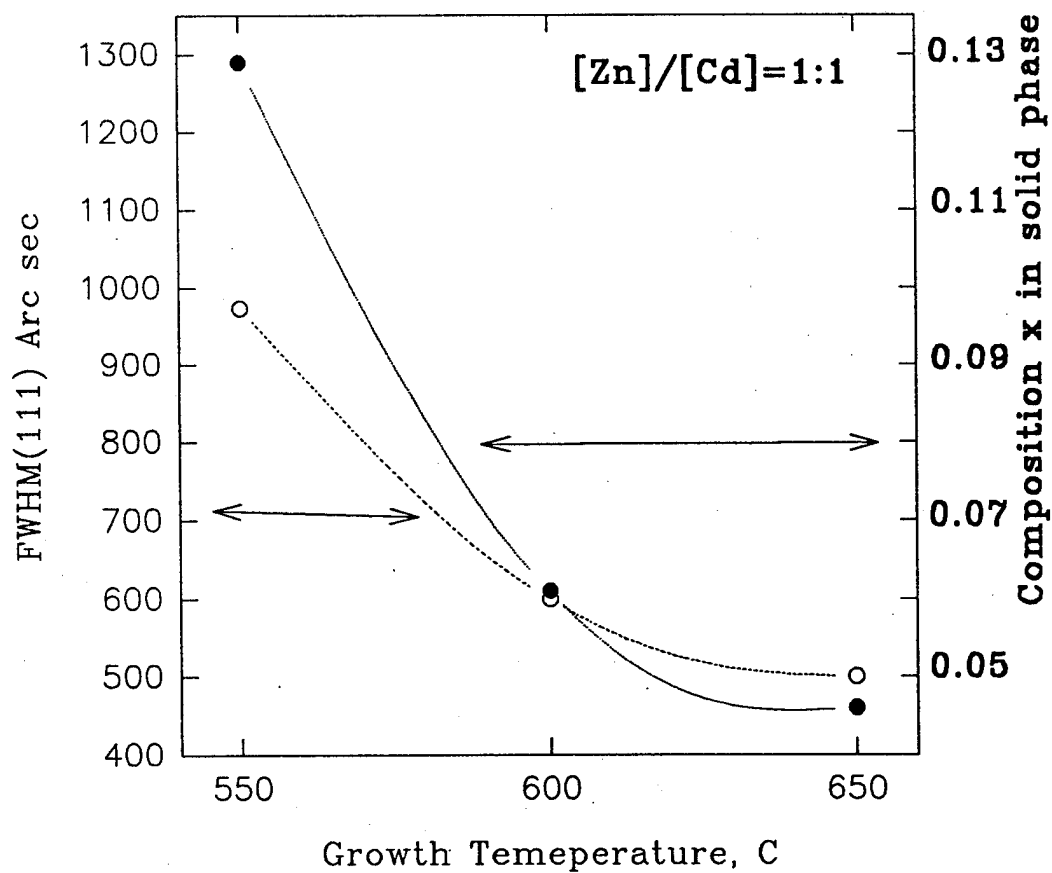
coefficient of Cd in $Zn_{1-x}Cd_xS$ is less than 1 at the conditions studied. For example, to lattice-match $Zn_{1-x}Cd_xS$ film to GaAs substrates, the composition variable x should be close to 0.60 while in the gas the DeZn/DMCd ratio should be maintained at 0.75.

The PL spectrum from the sample with x=0.40 was taken at 300 K and 77 K, using the 353 nm laser line from an Ar-laser, and is shown in Fig. V.2. Both room and low temperature measurements show a defect-related broad emission in the red-green region of the spectrum, while the two strong peaks at 385 and 415 nm observed in the 37 K PL spectrum are related to the alloy band gap. The band gap energy in the $Zn_{1-x}Cd_xS$ material is dependent on the composition x and theoretically can be vary from 3.6 eV for ZnS to 2.4 eV for CdS. Additional PL measurements are to be performed this month on samples with different amount of Cd in the $Zn_{1-x}Cd_xS$. In the next quarter we will enhance the band gap in these ZnS-based materials by adding Mg and create $(Zn_{1-x}Cd_x)_{1-y}Mg_yS$ alloys. If solid solutions can be formed, then the band gap in alloys lattice-matched to GaAs can be varied from 2.8 eV to about 4 eV, creating additional opportunities to optimize electronic properties of wave-guiding and cladding layers.

## MOCVD Growth of GaN on Gallate and Aluminate Substrates

During the past quarter, GaN growth has continued on the new lattice-matched substrates, $LiGaO_2$ and $LiAlO_2$ ($a_{GaN} = 3.189$ Å , $a_{LiGaO2} = 3.186$ Å, $a_{LiAlO2} = 3.134$Å). As mentioned in the previous report, the new substrates have a crystal structure similar to ZnO if one considers ZnO of the stoichiometry $ZnZnO_2$, with Li replacing one sublattice and Al or Ga replacing the other. Growth has been investigated at temperatures of 650, 700, and 750° C without the use of a low temperature buffer layer inherent to growth of GaN on sapphire and 6H-SiC substrates.

At 650°C, low resolution X-ray diffraction spectra only showed GaN peaks corresponding to (0002) and (0004) reflections, indicating high crystallinity. zHigher temperatures produced island-like growth with poor crystallinity. The poor quality has been attributed to thermal decomposition of the substrates.

More attention has been given to establish a better method for etching the novel substrates. A preliminary study was carried out to determine an adequate etching solution. Initially, a room temperature solution of a 3:1 H_2SO_4: H_3PO_4 solution seemed to be the best etching solution. However, after testing additional solutions, a 10 minute etch in *only* H_3PO_4 gave the best surface morphologies as observed by Nomarski optical microscopy. A more rigorous etching study will be conducted to provide more detailed indications of defect density and etching rate. A photoresist mask will be used to etch a step and its height will be measured using a Dektak profilometer to to determine etch rate. The Namarski microscope will be used to determine surface morphology.

Low temperature growth (< 850°C) on $LiGaO_2$, $LiAlO_2$, sapphire and 6H-SiC will be continued. Improvements in the quality of GaN at low temperatures are necessary for achieving high indium incorporation in ternary $In_xGa_{1-x}N$ films.

14

Fig. V.2. ZnCdS Thin Film Room temp. and 77K
353nm Excitation Ar Laser
475nm Pass filter >650nm
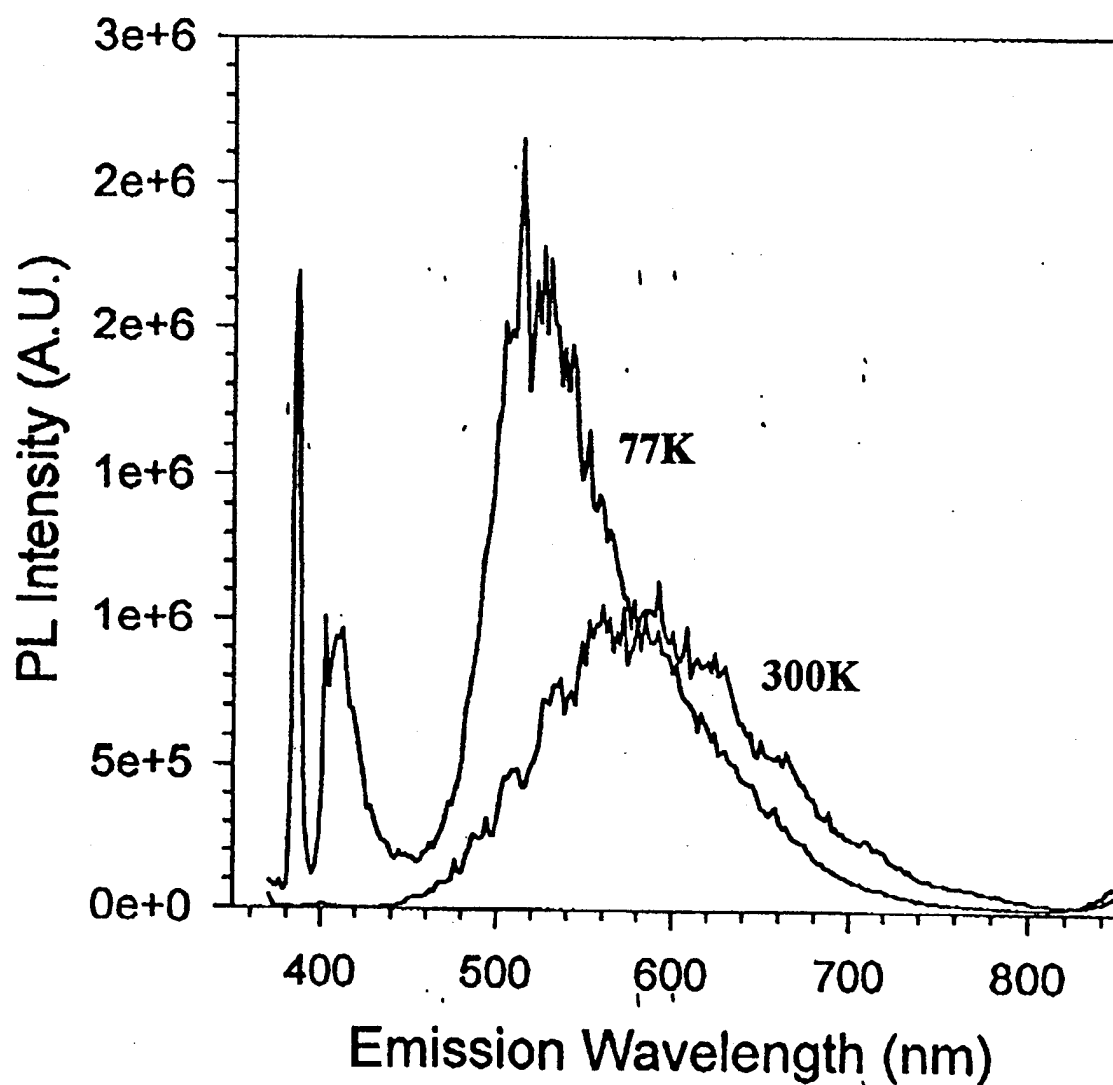
(VI)   Development of Diode Lasers (Peter Zory)

<u>ZnSe-Based Diode Laser Materials</u>

Two battery-driven (portable) electrochemical cells were built and CdZnSe quantum well laser material from 3M installed. The cells were used to demonstrate the liquid contact luminescence (LCL) technique, described previously, to various groups including those at ONR, AFOSR and the University of Maryland. The cells were also used during a presentation on the LCL technique at the blue-green diode laser session of the IEEE/LEOS Conference in San Francisco. LCL sample preparation and activation techniques were discussed with Paul Baude (3M) and an LCL sample with one-half of the cap area removed was delivered.

While the LCL technique has been shown to be non-destructive with red laser material, there is some deterioration of light output (from both red and green material) with running times exceeding about 15 minutes. In some cases, the original light output can be restored with a simple wafer cleaning procedure. If this "surface deterioration" problem can be solved, we intend to develop the LCL technique to the point where it can be utilized to "lifetest" unprocessed ZnCdSe laser material.

In a separate problem with production of ZnSe-based lasers, discussions have been held with M. Haase of 3M with respect to an epi-side-down solder yield problem. Samples of GaAs quantum well laser material, processed at UF, have been sent to 3M to determine if they show the same problem.

<u>GaN-Based Materials</u>

Work is continuing on the development of a grating-coupled/distributed feedback DH GaN/AlGaN diode laser. Threshold gain versus mode frequency curves have been generated for the 0-reflectivity end case. The more realistic problem involving distributed end reflectors is now being addressed.

(VII)   Theoretical Calculations of Dopants of ZnSe (Gertrude Neumark)

Analysis of the temperature dependence of the deep PL bands observed in heavily N-doped ZnSe showed that the intensity of the DAP bands decreased with an activation energy of about 40 meV. This is, within experimental error, the same value as reported by Hauksson, et al., (Appl. Phys. Lett **61** (1992), 2208) for the deep donors observed at intermediate doping. This result shows that the compensating donors in very heavily N-doped ZnSe are the same as those obtained at intermediate doping.

Further studies of screening confirmed that this effect becomes increasingly important with higher doping. Table 1 gives our results from an analysis of literature data (Fan, et al., J. Crystal Growth, **138**, (1994), 464, and Han, et al., J. Electronic Materials, **23**, (1994), 245) as well as the values of N_A, N_D, and E_A obtained in those papers via the "standard" analysis, which assumes E_A independent of temperature. It can be seen that the differences increase with increasing doping. E_{AO} in our analysis is the value of E_A in the absence of screening.

Table VII.1. Electrical Properties of ZnSe:N

	N_A $(10^{17}$ cm$^{-3})$	N_D $(10^{16}$ cm$^{-3})$	$N_A - N_D$ $(10^{17}$ cm$^{-3})$	E_{AO} (meV)	E_A(RT) (meV)
Fan, et al	0.776	0.692	0.707	106*	106*
present work	0.670	0.650	0.650	112	99.8
Han, et al	9.54	10.10	8.53	92*	92*
present work	6.80	7.10	6.09	112	81.5

*   Constant as a function of temperature.

A further interesting aspect, related to the deep PL of the heavily N-doped ZnSe, is that the screening length obtained from the fluctuation model (Kothandaraman, et al., Appl. Phys. Lett., **67**, (1995), 3307) is about a factor of three smaller than the one which would be obtained for an equivalent "standard" (Brooks-Herring type) screening model. We believe that this indicates non-equilibrium dopant incorporation. This model is corroborated by comparing literature results of N implantation into bulk ZnSe, which gave voids (Vermaak & Petruzzello, J. Electronic Materials, **12**, (1983) 29), with recent MBE results.

(VIII) MOCVD Growth of GaN (Jacques Pankove)

Efforts this quarter have continued to be placed on studying the gap-states in gallium nitride thin films. We have extended our photoconductivity spectroscopy measurements with a number of samples, including "high quality" unintentionally doped n-type GaN with high room temperature mobility. This film showed features similar to previously measured high mobility samples, including a long exponential tail of states far into the gap and a steeper region near the band edge. We are currently in the process of compiling and analyzing the data taken to date.

We have noticed that in the photoconductivity spectrum of some samples, there is a bulge in the 2.0-2.7eV range of photon energies (Fig. VIII.1.). To further explore this phenomenon, we acquired two pieces of the normalized photoconductivity spectra for the two samples. Notice that below 3.2eV, sample CQ6153 shows only the exponential dependence of photoconductivitiy, while sample CQ615 displays the bulge around 2.2-2.5eV. Because the position of this bulge is similar to the peak emission from the yellow luminescence commonly observed in photoluminescence spectra, the room temperature photoluminescence spectra of these two samples were measured and are compared in Fig. VIII. 2. It is clear that sample CQ615 which showed the bulge in the PC spectrum also displays a stronger yellow luminescence peak. This apparent correlation will be explored further. More samples will be measured to determine if the states responsible for the PC spectrum bulge are the same states responsible for the yellow peak in PL spectra.
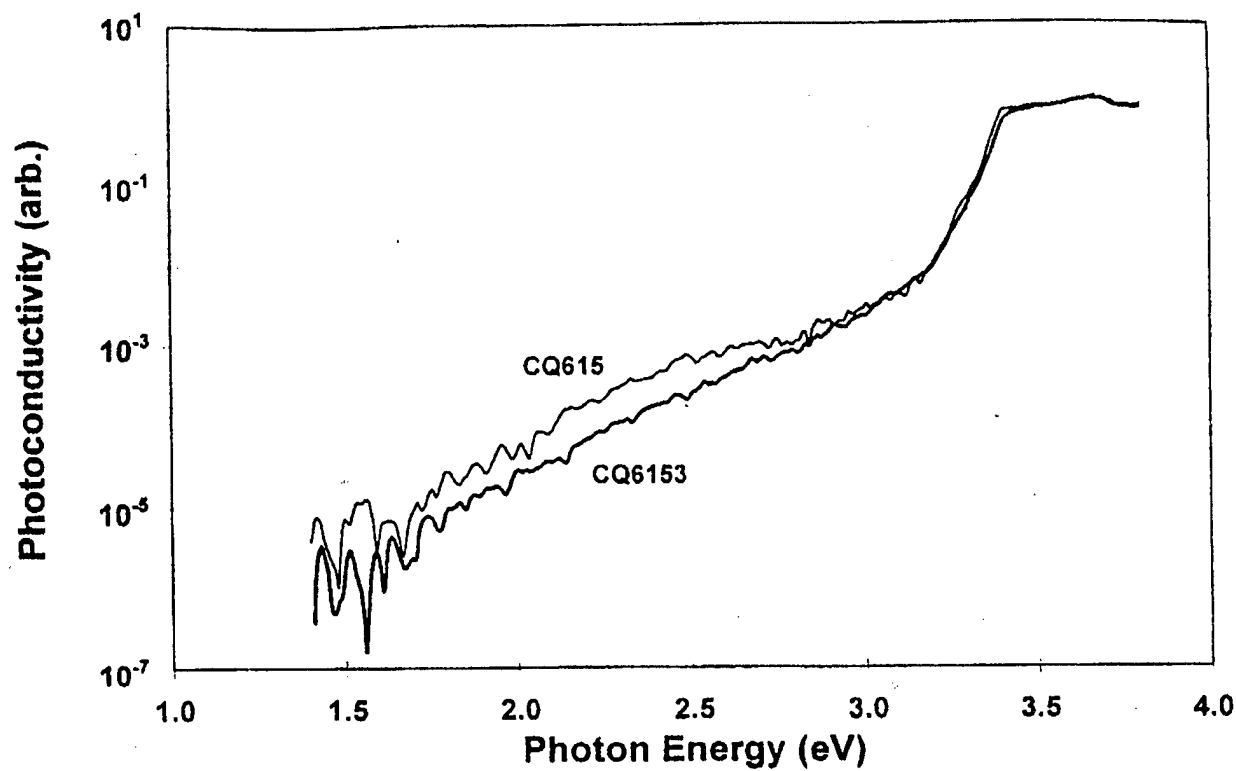
Fig. VIII.1. Normalized photoconductivity spectra for undoped
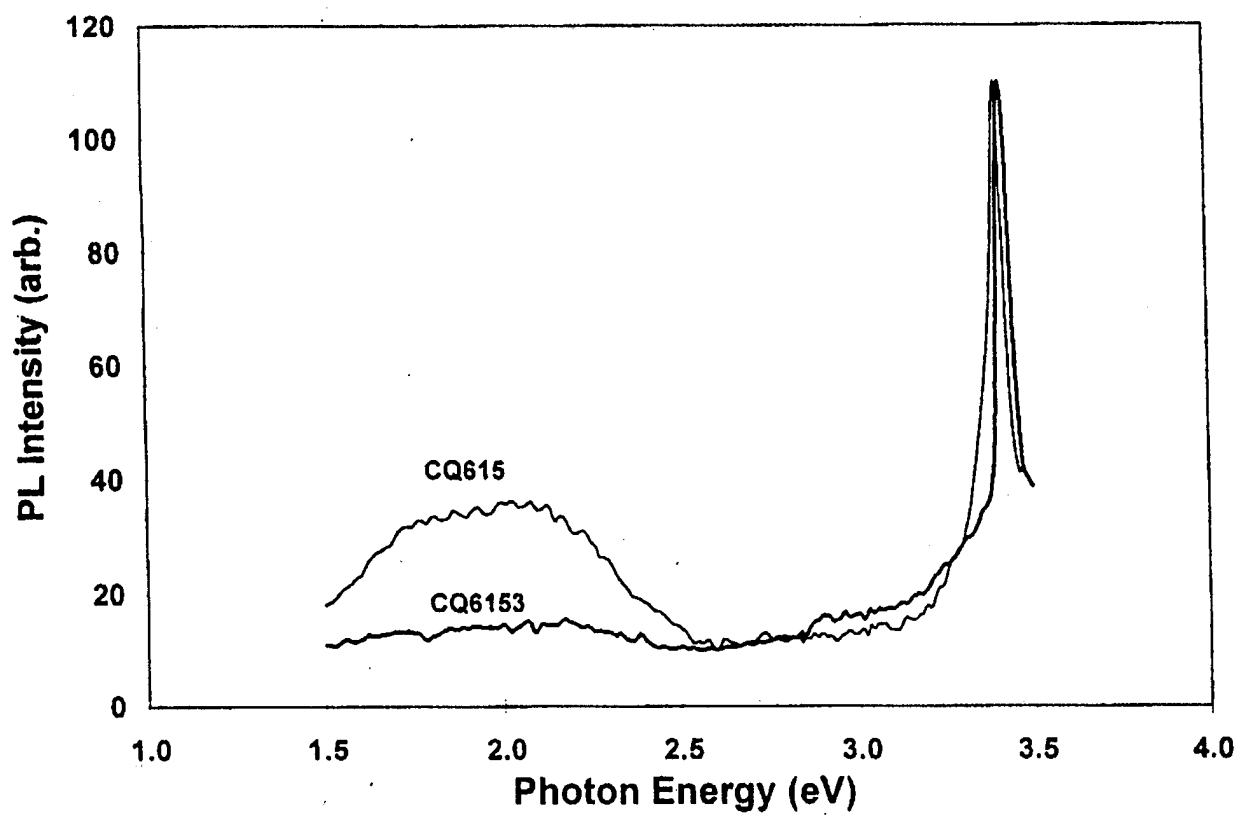GaN samples CQ615 and CQ6153

Fig. VIII.2. Normalized photoluminescence spectra for undoped
GaN samples CQ615 and CQ6153

(IX)   Gain Modeling in II-VI Strained-Layer QW Structures
Reinhart Engelmann)

Further two-dimensional studies have been performed using the simulation software package SILVACO. The effect of stripe width in gain-guided II-VI SCH QW lasers was studied. Threshold and mode patterns were determined for stripe widths ranging from 3 to $20\mu m$; gain hole burning with mode self-focusing was observed for $50\mu m$ stripe width.

Two-Dimensional (2D) Lasing Simulation

We have applied the 2-D modeling procedure described in our previous report for additional simulations of blue-green II-VI laser structures, particularly for investigating the influence of the stripe width on the laser performance. Fig. IX.1 demonstrates the influence of the stripe width on the fundamental mode pattern. As can be seen, the width of the mode decreases less strongly than the width of the stripe, W. For $W = 20\mu m$, the mode is considerably smaller than W. For $W = 10\mu m$, the mode size approaches W, and at $W = 5\mu m$ the mode becomes larger than W. In the latter case the mode size is mainly determined by lateral current spreading and carrier diffusion. Thus, threshold current tends to saturate for stripe widths below $5\mu m$, as demonstrated in Fig. IX.2. At large W, the mode size is governed by gain hole burning which generates a self-focusing effect and reduces the mode size. This effect is shown in Fig. IX.3 for $W = 50\mu m$. Due to self-focusing, the lateral mode size is only marginally larger than at $W = 20\mu m$. (Note the different scales when comparing Figs. IX.1 and IX.3.) The results are very consistent with what is known from gain-guided lasers of the III-V materials systems, i.e. independent of stripe width, the lateral mode size remains in the neighborhood of about $10\mu m$.

Future Plans

Major advancements of LED performance with violet, blue, green and yellow emission has recently been achieved by Nichia Chemical Industries in Japan based on nominally undoped single quantum well (SQW) InGaN diode structures [1-3]. External quantum efficiencies are consistently above 1% and are close to 10% for blue emission. These are highly remarkable achievements and pave the way for InGaN QW diode lasers. We intend to analyze the reported data for application to SQW laser modeling in this material system.

REFERENCES:

[1]   S. Nakamura, M. Senoh, N. Iwasa, and S. Nagahama, "High-brightness InGaN blue, green and yellow light-emitting diodes with quantum well structures," Jpn. J. Appl. Phys. 34, Part 2 (7A), pp. L797-L799 (1 July 1995).

[2]   S. Nakamura, M. Senoh, N. Iwasa, and S. Nagahama, "High-power InGaN single-quantum-well-structure blue and violet light-emitting diodes," Appl. Phys. Lett. 67 (13), pp. 1868-1870 (25 September 1995).

[3]   S. Nakamura, M. Senoh, N. Iwasa, S. Nagahama, T. Yamada, and T. Mukai, "Superbright green InGaN single-quantum-well-structure light-emitting diodes," Jpn. J. Appl. Phys. 34, Part 2 (10B), pp. L1332-L1335 (15 October 1995).
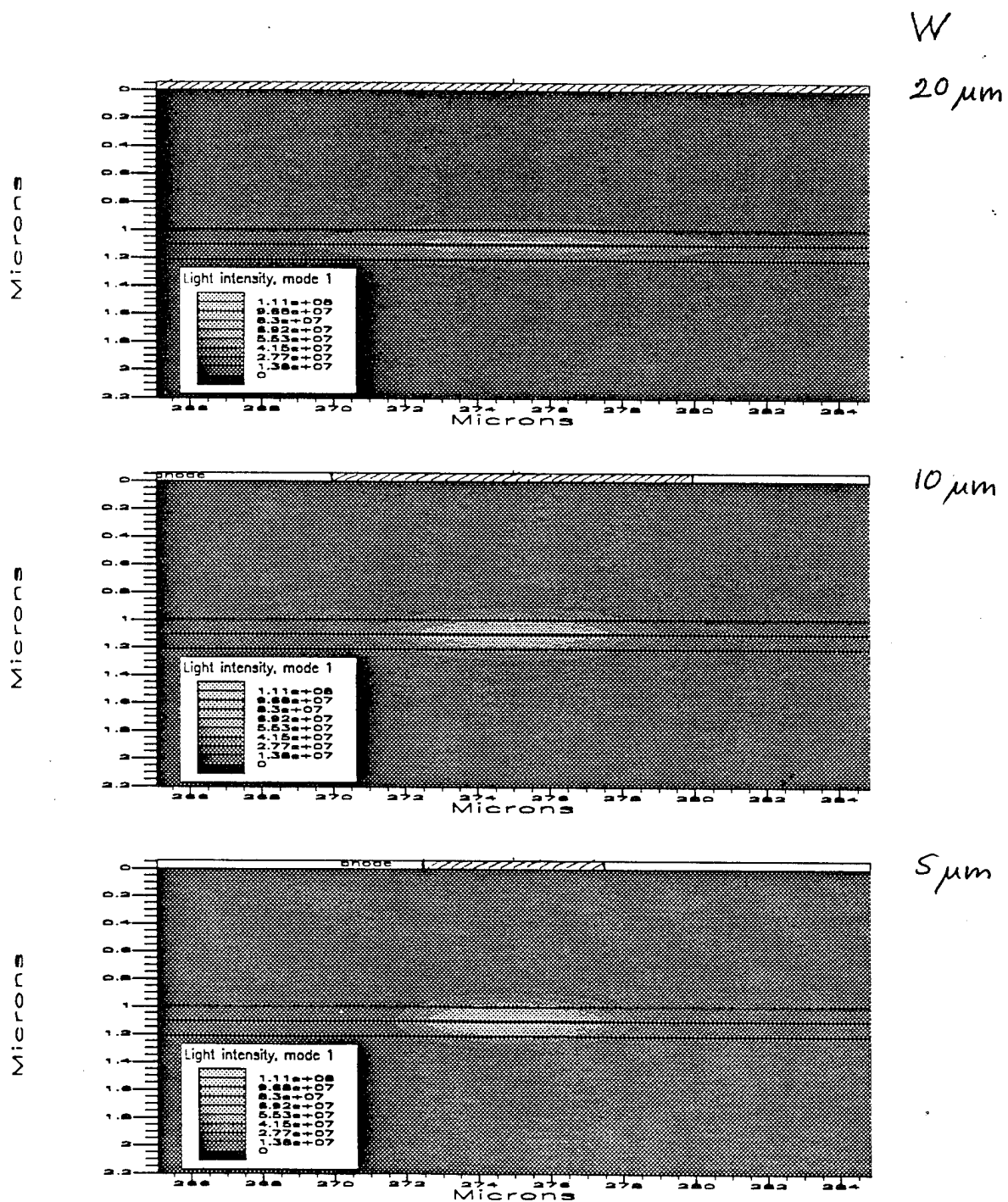
W

$20\,\mu m$

$10\,\mu m$

$5\,\mu m$

Fig. IX.1.   Mode Patterns vs. Stripe Width W.

Threshold current vs. stripe width W (1 mm cavity length)
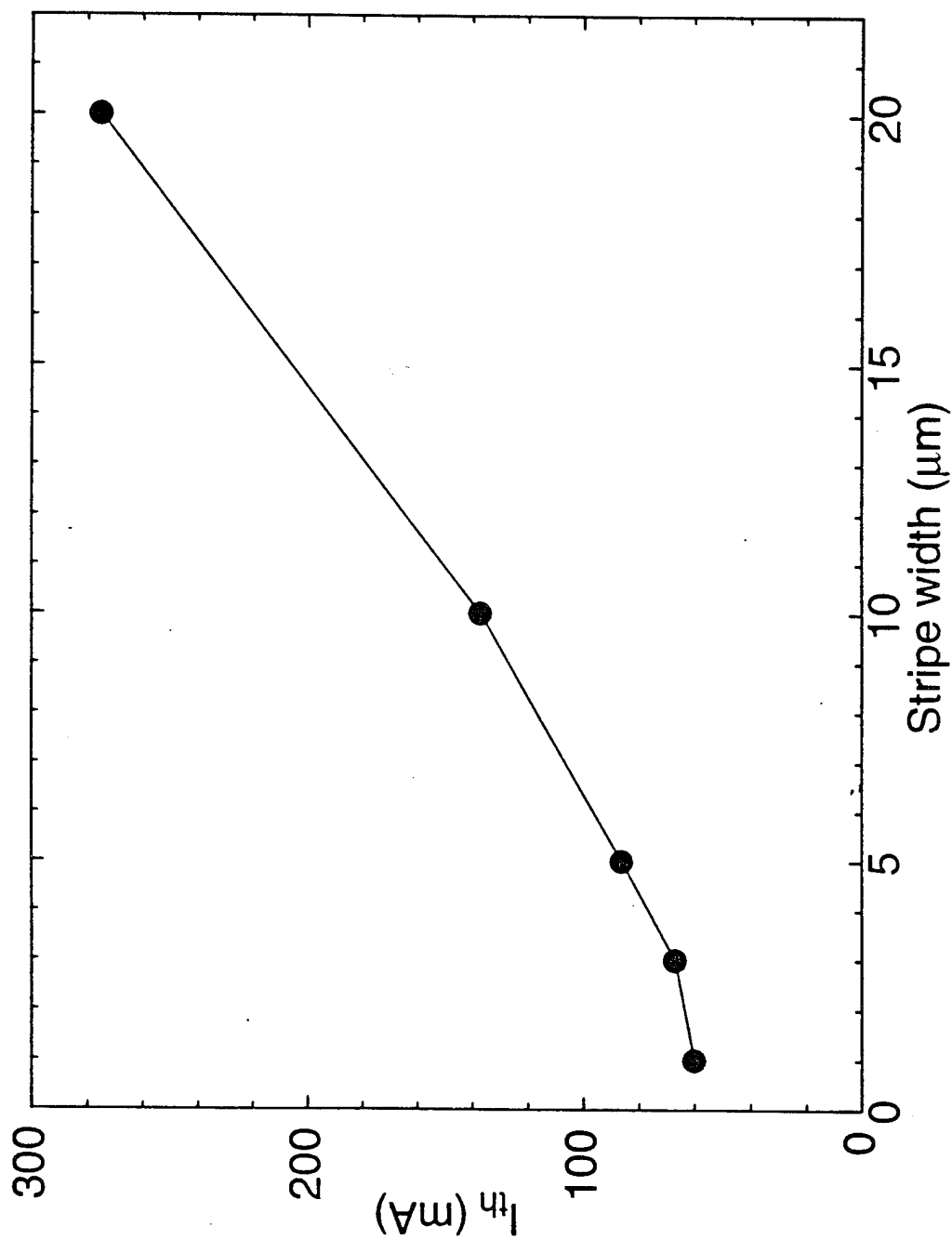
Fig. IX.2.

Self-Focusing of Device with Wide Stripe
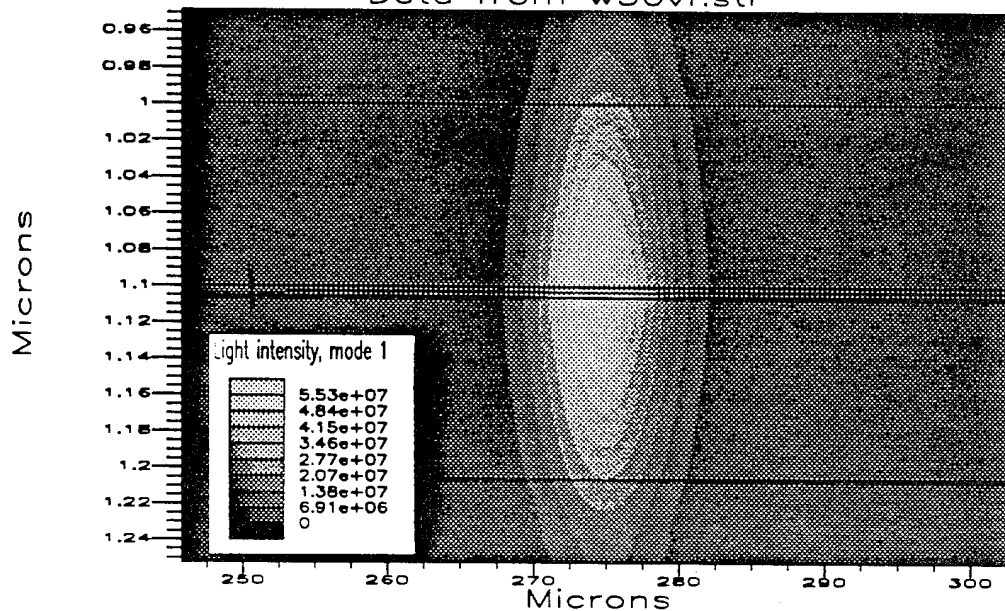## (W = 50mm)

ATLAS
Data from w50vf.str
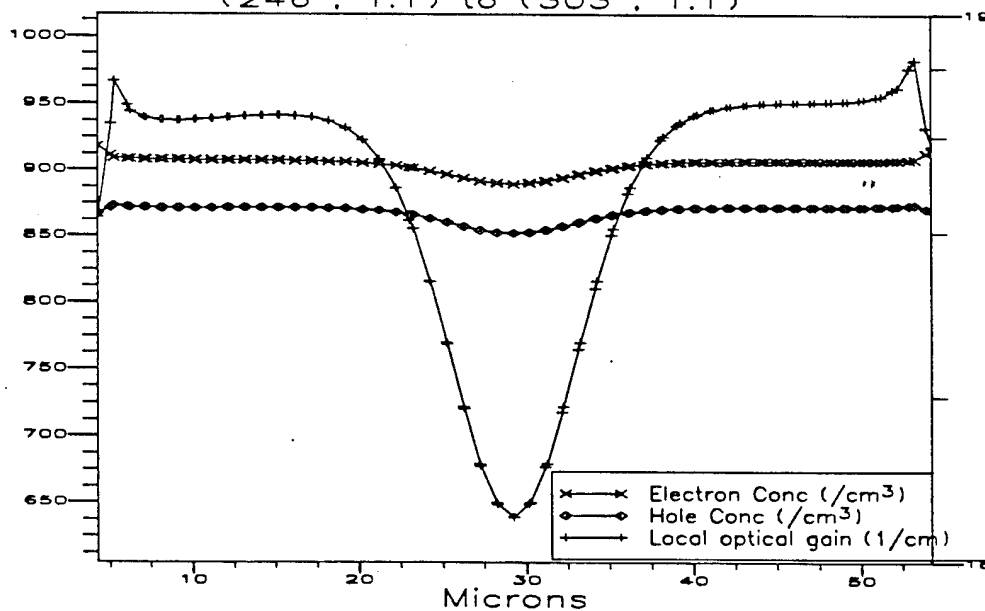

Section 1 from w50vf.str
(246 . 1.1) to (303 . 1.1)

Fig. IX.3.

PUBLICATIONS:

Dissertations
- Y. Cai , "Wide-band-gap II-VI semiconductor heterostructure Modeling and device design." Ph.D. Dissertation, Oregon Graduate Institute of Science and Technology, Nov. 1995.

- John J. Fijol, "Electrical Contacts to p-Type ZnSe", PhD Dissertation, University of Florida, Dec. 1995.

Papers
- Li Wang and Joseph H. Simmons, "Observation of exciton and biexciton processes in $Cd_xZn_{1-x}Se/ZnSe$ (x = 0.2)," Appld. Phys. Lett. **67** (10), p.1450, Sept. 4, 1995.

- I. Kuskovsky, G.F. Neumark, Proc., MRS, submitted., C. Kothandaraman, G.F. Neumark, R.M. Park., Appl. Phys. Lett., **67**, (1995), 3307.

- C. Kothandaraman, G.F. Neumark and R.M. Park, J. Crystal Growth, in press.

PRESENTATIONS
- C. McCreary, A. Davydov, E. Bretschneider, and T. Anderson , "MOCVD Growth of ZnS using methyl mercaptan as an alternate sulfur source," AIChE 1995 Annual Meeting, Maimi-Beach, Florida, November 12-17. Abstract p. 160.

- A. Ahmed, Z. Osman, T. Dann, and T. Anderson, " Growth and Characterization of MOCVD of GaN," presented at the national AIChE conference in Miami Beach, Florida on November 14.

- In conjunction with the IEEE/LEOS Distinguished Lecturer ward, Peter Zory made presentations at the following locations:
    o   University of Toronto in Toronto, Canada, Sept. 22, 1995;
    o   National Research Council in Ottawa, Canada, Sept. 25, 1995;
    o   Sarnoff Research Center in Princeton, NJ, Sept. 28, 1995;
    o   University of Maryland in College Park, MD, Oct. 17, 1995;
    o   Old Dominion University in Norfolk, VA, Oct. 20, 1995; and
    o   University of California in Davis, CA; Nov. 2, 1995

- P.S. Zory, C.L. Young, C.F. Hsu, J.S.O and C.C. Largent "Diode Laser Material Evaluation Using Liquid Contact Luminescence" IEEE-LEOS Conference, San Francisco, CA, 1 Nov. 95.

- I. Kuskovsky, G.F. Neumark, Fall 1995 MRS Meeting,

- I. Kuskovsky, G.F. Neumark, to be presented, APS, March '96.

Presentations: (Continued)

- J. T. Trexler, S.J. Miller, P.H. Holloway, and A. Kahn, "Reactions Between Au/Ni Thin Films and p-GaN," 42nd National Symposium of the American Vacuum Society, Minneapolis, MN, October 16-20, 1995.

- J. Trexler, J. Fijol, L. Calhoun, R. Park, and P. Holloway, "Electrical Contacts to p-ZnTe," Seventh Intl. Conf. on II-VI Compounds and Devices, August 13-18, 1995, Edinbrough, Scotland.

- J.T. Trexler, S.J. Miller, P.H. Holloway and A. Kahn., "Interfacial Reactions between Metal Thin Films and p-GaN", Fall Meeting of the MRS, Boston, MA, November 27-Dec. 1, 1995.

- A. Durba, S.J. Pearton, C.R. Abernathy, P. H. Holloway and F. Ren, "WSi$_x$ Ohmic Contacts on InGaN",. Fall Meeting of the MRS, Boston, MA, November 27-Dec. 1, 1995.

- Paul H. Holloway, J. F. Fijol, and J. T. Trexler, "Ohmic Electrical Contacts to ZnSe Diode Lasers,"Joint TMS/Japanese Institute of Metals Symposium on Advanced Materials and Technology for the 21st Century, Honolulu, Hawaii, December 13-15, 1995, INVITED TALK.

Post Doctoral Associates, Graduate Research Assistants, and Undergraduate Research Assistants:

Post Doctoral Associates:

Akhter Ahmed with Dr. Anderson
Ziad Osman with Dr. Anderson
Viswananth Krishnamoorthy with Dr. Jones
Chang-hua Qiu with Dr. Pankove

Graduate Research Assistants:

Bruce Liu with Dr. Park
Minyon Jeon with Dr. Park
George Kim with Dr. Park
K.N. Lee with Dr. Abernathy
Jin Hong with Dr. Pearton
Jeff Hsu with Dr. Zory

Graduate Research Assistants: (Continued)

Jason O with Dr. Zory
Igor Kuskovskiy with Dr. Neumark
Li Wang with Dr. Simmons
Y. Cai with Dr. Engelmann
William A. Melton with Dr. Pankove
John Fijol with Dr. Holloway
T.J. Kim with Dr. Holloway
Jeff Trexler with Dr. Holloway
Eric Bretschneider with Dr. Anderson
Joe Cho with Dr. Anderson
Todd Dan with Dr. Anderson
J. Kim with Dr. Jones
S. Bharatan with Dr. Jones
S. Bhendi with Dr. Jones

Undergraduate Research Assistants:

Julie Sauer with Dr. Simmons
Bob Covington with Dr. Anderson
Michael Mui with Dr. Anderson
Brendon Cornwell with Dr. Anderson

f:uridec02.doc

Observation of exciton and biexciton processes in Cd$_x$Zn$_{1-x}$Se/ZnSe (x=0.2)

Li Wang and Joseph H. Simmons[a]

Department of Materials Science and Engineering, University of Florida, Gainesville, Florida 32611

Exciton and biexciton transitions have been observed in low-temperature (10 K) photoluminescence from Cd$_x$Zn$_{1-x}$Se/ZnSe (x=0.2) multiple quantum well samples grown by molecular beam epitaxy. Transient photoluminescence experiments were conducted to study the dynamics of carrier decay associated with these processes. The formation of exciton and biexciton species is confirmed by examining their energy positions, intensity dependence on excitation power density, spectral line shapes, relative decay lifetimes, and polarization dependence. © 1995 American Institute of Physics.

Semiconductor quantum well structures have nonlinear optical properties that are strongly dominated by excitonic resonances near the band gap. Investigating the physics of excitonic processes in quantum structures is essential to both understanding the fundamental behavior of quantum confined carriers and determining their role in potential device applications. At low temperatures, excitons are formed by electron and hole pairs bound together by Coulomb interaction. In the limit of low nonequilibrium density, the exciton gas can be considered as a weakly interacting Boltzmann gas, however, in the limit of high nonequilibrium density, excitons can condense to form excitonic molecules, also called biexcitons.[1] The enhancement of biexciton binding energy due to quantum confinement makes observation of biexcitons less difficult at low temperatures. The biexciton line has been observed in II–VI semiconductors with binding energies in the range of 1–10 meV.[2-5] Since biexcitons are formed by two interacting excitons with opposite spins, the biexciton photoluminescence intensity is expected to increase superlinearly with respect to the exciton, and the recombination lifetime of biexcitons should be about half that of excitons. Also, the line shape of biexcitons in direct band-gap semiconductors is distinguished by a reverse (or inverse) Boltzmann-like distribution due to momentum conservation during the biexciton recombination process.[6] The recombination of biexcitons involves the emission of a photon $\hbar\omega_B$, leaving a free exciton, as follows:[7]

$$h\nu_B = E_g - E_x - E_B + E_{xk} + E_{Bk},\qquad(1)$$

where E_x and E_B are the binding energies of the exciton and biexciton, respectively, E_g is the energy gap, and E_{xk} and E_{Bk} are kinetic energies of the exciton and biexciton, respectively. Finally, the 2-photon coherence nature of biexciton transitions leads to a unique polarization selection rule, whereby two cross-circularly polarized beams will induce a biexciton transition while cocircularly polarized beams will not.[8]

In this letter, we report the observation of exciton and biexciton transitions at 10 K in quantum well structures with Cd$_{0.2}$Zn$_{0.8}$Se as the well material and ZnSe as the barrier

material. The samples were grown on GaAs substrates by molecular beam epitaxy. Their structures consist of a 2 μm ZnSe buffer layer on GaAs, followed by 10 periods of un-doped multiple quantum wells with a ZnSe barrier thickness of 100 Å and a CdZnSe well thickness of 50 Å. Steady state and transient photoluminescence measurements were con-ducted with an exciton source consisting of an amplified, frequency-doubled, mode locked Ti:sapphire laser (400 nm, 300 fs, 250 kHz, 2.4 μJ/pulse). Population mixing (or corre-lation excitation spectroscopy)[9] as described in another publication[10] was used to measure carrier recombination life-times. In this technique, two pulse trains from the above source are chopped at different frequencies and focused onto the sample. The cross-correlation luminescence signal at the sum or difference frequency with respect to the time delay between the two pulse trains gives the decay lifetime.[9] The samples were maintained at 10 K in a closed cycle helium cryostat. The temporal resolution of the experimental system is determined by the pulse duration of the laser (300 fs). The beam was focused to 500 μm on the sample, which corre-sponds to an excitation power density of 20 W/cm^2.

Figure 1 is the photoluminescence spectrum of the MQW sample. Two major peaks are evident. We attribute the high energy peak to the free-exciton transition, and the lower
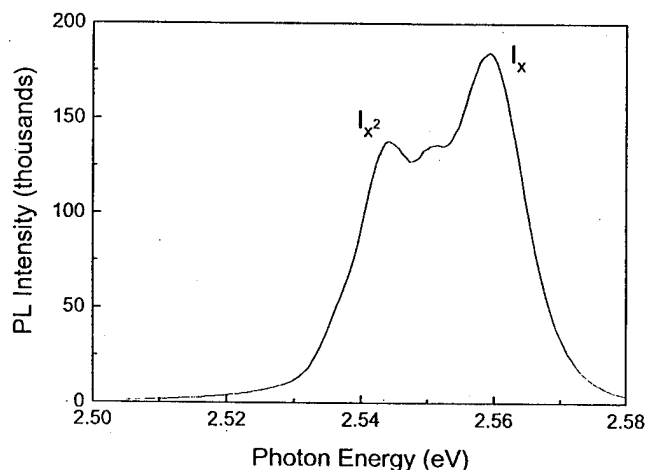

FIG. 1. 10 K PL spectrum of Cd$_{0.2}$Zn$_{0.8}$Se/ZnSe MQW sample with an excitation intensity of 2.4 μJ/pulse.
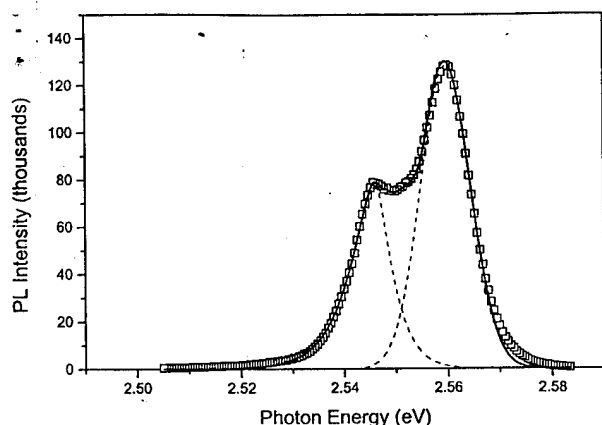
[a] Electronic mail: simmons@silica.mse.ufl.edu

FIG. 4. Theoretical fit to the PL spectrum from the 1 μJ/pulse excitation intensity. Empty squares represent the data; solid lines show the fit. The fitted exciton and biexciton line shapes are also shown separately in dashed lines.

responsible for those processes[18] were used in fitting this region. Figure 4 shows the fitted spectrum for the 1 μJ/pulse excitation intensity, and agrees well with the experimental data. The biexciton binding energy was estimated to be 10 meV from the fit, which agrees well with biexciton binding energies obtained from similar samples.[19,20]

In summary, we have observed exciton and biexciton lines in $Cd_{0.2}Zn_{0.8}Se/ZnSe$ MQW structures in low-temperature photoluminescence. The assignment of exciton and biexciton transitions was verified by examining their energy positions, intensity dependence on excitation density, relative decay lifetimes, excitation polarization dependence, and spectral line shapes. The experimental data agree well with current theories on exciton and biexciton formation.[12,22]

The authors would like to thank Dr. Robert Park and M. H. Jeon for providing the high quality MBE samples. This

[1] M. A. Lampert, Phys. Rev. Lett. **1**, 450 (1958).
[2] A. D. Kepner, K. I. Kang, Y. Z. Hu, S. V. Gaponenko, S. W. Koch, and N. Peyghambarian, Int. Quantum Electron. Conf. **9**, 135 (1994).
[3] K.-H. Pantke, J. Erland, and J. M. Hvam, J. Cryst. Growth **117**, 763 (1992).
[4] S. Charbonneau, M. L. W. Thewalt, M. Isshiki, and K. Masumoto, Solid State Commun. **67**, 187 (1988).
[5] S. Charbonneau, Opt. Eng. **28**, 1101 (1989).
[6] K. Cho, Opt. Commun. **8**, 412 (1973).
[7] A. Mysyrowicz, A. Gun, J. B. Levy, R. Biras, and A. Nikitine, Phys. Rev. Lett. **26A**, 615 (1968).
[8] H. Wang, J. Jagdeep, T. C. Damen, and L. N. Pfeiffer, Solid State Commun. **91**, 869 (1994).
[9] D. Rosen, A. G. Doukas, Y. Budansky, A. Katz, and R. R. Alfano, Appl. Phys. Lett. **39**, 935 (1981).
[10] L. Wang and J. H. Simmons (unpublished).
[11] H. Wang, K. B. Ferrio, D. G. Steel, Y. Z. Hu, R. Binder, and S. W. Koch, Phys. Rev. Lett. **71**, 1261 (1993).
[12] S. Schmitt-Rink, D. Bennhardt, V. Heuckeroth, P. Thomas, P. Haring, G. Maidorn, H. Bakker, K. Leo, D. S. Kim, J. Shah, and K. Koehler, Phys. Rev. B **46**, 10460 (1992).
[13] S. Bar-Ad, I. Bar-Joseph, G. Finkelstein, and Y. Levinson, Phys. Rev. B **50**, 18375 (1994).
[14] D. J. Lovering, R. T. Phillips, G. J. Denton, and G. W. Smith, Phys. Rev. Lett. **68**, 1880 (1992).
[15] S. Bar-Ad and I. Bar-Joseph, Phys. Rev. Lett. **68**, 349 (1992).
[16] K. H. Pantke, D. Oberhauser, V. G. Lyssenko, J. M. Hvam, and G. Weimann, Phys. Rev. B **47**, 2413 (1993).
[17] S. Shionoya, H. Saito, E. Hanamura, and O. Akimoto, Solid State Commun. **12**, 223 (1973).
[18] S. Nikitine, in *Excitons at High Density*, edited by H. Haken and S. Nikitine (Springer, Berlin, 1975).
[19] M. Lowisch, F. Kreller, J. Puls, and F. Henneberger, Phys. Status Solidi B **188**, 165 (1995).
[20] Y. Yamada, T. Mishina, Y. Masumoto, Y. Kawakami, S. Yamaguchi, K. Ichino, S. Fujita, S. Fujita, and T. Taguchi, Phys. Rev. B **51**, 51 (1995).
[21] A. L. Ivanov and H. Haug, Phys. Rev. B **48**, 1490 (1993).
[22] C. Klingshirn and H. Haug, Phys. Rev. Rep. **70**, 315 (1981).